THEORY OF THRESHOLD FLUCTUATIONS IN NERVES

I. Relationships between Electrical Noise and Fluctuations in Axon Firing

HAROLD LECAR *and* RALPH NOSSAL

From the Laboratory of Biophysics, National Institute of Neurological Diseases and Stroke, and the Physical Sciences Laboratory, Division of Computer Research and Technology, National Institutes of Health, Bethesda, Maryland 20014

ABSTRACT Relations describing threshold fluctuation phenomena in nerves are derived by calculating the approximate response of the Hodgkin-Huxley (HH) axon to electrical noise. We use FitzHugh's reduced phase space approximation and describe the dynamics of a noisy nerve by a two-dimensional brownian motion. The theory predicts the functional form and parametric dependence of the relation between probability of firing and stimulus strength. Expressions are also obtained for the firing probability as a function of stimulus duration and for the distribution of latency times as a function of stimulus strength.

I. INTRODUCTION

The random firing of nerve cells exposed to near-threshold stimuli has been studied for many years (Blair and Erlanger, 1932; Monnier and Jasper, 1932; Pecher, 1939; Ten Hoopen and Verveen, 1963). Although the statistical characteristics of these firing fluctuations have been the subject of a number of theoretical discussions (Landahl, 1941; Stein, 1967; Gastwirth, 1967), the underlying physical origin of the phenomenon still remains obscure. Recently, there have been several studies of electrical noise in resting nerve axons (Verveen and Derksen, 1968; Poussart, 1969) which give information about the fundamental noise sources of the excitable membrane. In this paper we establish the theoretical connection between the probabilistic firing of axons and the electrical noise generated across the nerve membrane. The aim of our analysis is to relate such excitability fluctuations to the physical conductance mechanisms in the membrane.

Our analysis is based on the HH system of differential equations describing nerve excitation (Hodgkin and Huxley, 1952; Frankenhaeuser and Huxley, 1964). These equations are exceedingly difficult to analyze exactly, and we shall therefore confine

our attention to an approximation in which two of the HH variables are ignored. This reduced set of equations, introduced by FitzHugh (1961), allows us to study the threshold phenomenon in terms of trajectories in a two-dimensional phase plane.

In order to establish the relation between threshold fluctuations and electrical noise, we introduce noise sources into the equation and study the resultant brownian motion in the phase plane. The various noise sources are represented by Langevin forces (Lax, 1966). The firing fluctuations are obtained from the probability distribution for the values of voltage and conductance which the system attains after stimulation.

II. THRESHOLD PROPERTIES AS CALCULATED FROM THE *Vm* REDUCED SYSTEM

We wish to consider the threshold properties of the empirical equations for the electrical characteristics of a region of axon membrane. Generally, we will refer to the set of differential equations as the HH equations, although we will often be concerned with the modified system of equations derived by Frankenhaeuser and Huxley (FH) for the node of Ranvier of the toad sciatic nerve (Frankenhaeuser and Huxley, 1964).

The empirical equations have the following form:

$$C\frac{dV}{dt} = I - I_i, \tag{1}$$

where I is the external stimulating current and I_i is the ionic current across the membrane. The ionic current has been described somewhat differently for different nerve preparations. For example, the original form given by Hodgkin and Huxley (1952) for the squid giant axon is:

$$I_i = g_K n^4(V - V_K) + g_L(V - V_L) + g_{Na} m^3 h(V - V_{Na}), \tag{2a}$$

whereas the equation used by Frankenhaeuser and Huxley (1964) for the node of Ranvier has the form:

$$I_i = P_K n^2 f(V - V_K) + g_L(V - V_L) + P_{Na} m^2 h f(V - V_{Na}) + P_p p^2 f(V - V_p). \tag{2b}$$

These equations do not differ in any significant details. As compared with the HH equations, the FH equations contain a small additional component of current. Also, different power laws are employed to reproduce the observed time-delay kinetics, and the instantaneous current-voltage relation is represented by the constant-field form $f(V - V_i)$ (Goldman, 1943) instead of the HH linear form. In both sets of equations, the variables m, n, and h describe the relaxation of the voltage-dependent

conductances. These variables all obey subsidiary equations of the form,

$$\frac{dv}{dt} = [1/\tau_v(V)][v_\infty(V) - v]\,; v = m, h, n, p\,. \qquad (3)$$

Here $\tau_v(V)$ is a voltage-dependent time constant and $v_\infty(V)$ is related to the steady-state, voltage-dependent value of the parameter in question.

The *Vm* approximation (FitzHugh, 1961) consists of setting the variables n and h equal to their resting values and solving the remaining pair of equations for V and m. Under certain conditions this procedure gives a good approximation to the sub-threshold and near-threshold behavior of the system. The separation is possible because V and m (excitation variables) characteristically vary more rapidly by an order of magnitude than do n and h (recovery variables). Typical solutions of the *Vm* and HH equations for near-threshold stimuli are shown in Figs. 1 *a*–1 *c*. Because of the absence of recovery, the *Vm* solutions for "action potentials" do not return to the resting state. Rather, they give plateau responses to a fixed voltage, as shown in Fig. 1 *c*.

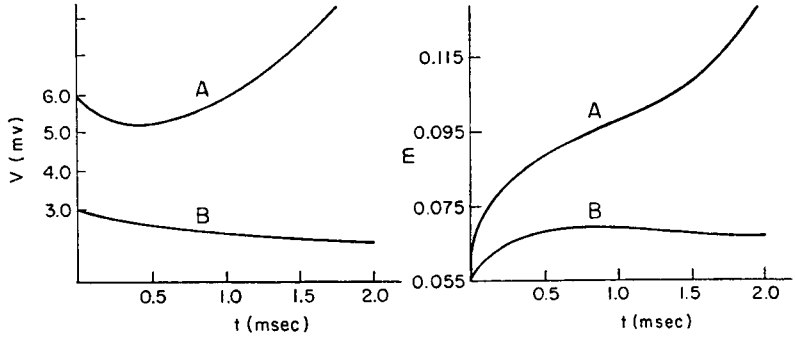

FIGURE 1 *a* Typical solutions for the *Vm* reduced equations for initial conditions below threshold *B* and above threshold *A* for the squid giant axon. These initial conditions result from a strong short current pulse.

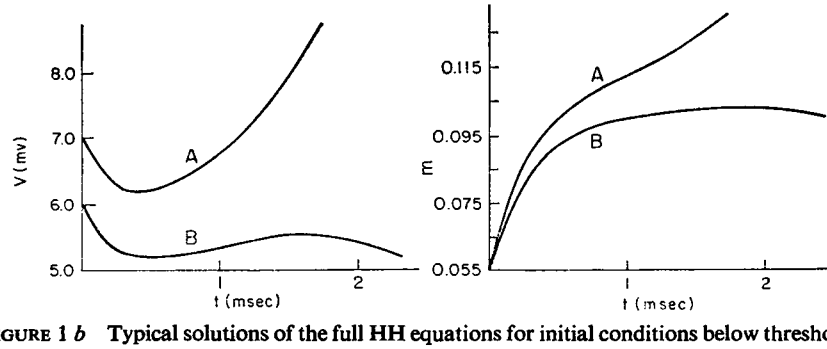

FIGURE 1 *b* Typical solutions of the full HH equations for initial conditions below threshold *B* and above threshold *A*.

The threshold properties of the *Vm* reduced system are most clearly seen in the phase-plane representation, as shown in Fig. 2. The reduced system phase trajectories fall into two classes separated by a limiting trajectory called the threshold separatrix. As has been discussed by FitzHugh (1969), the *Vm* and HH systems differ topologically, having different types of singular points. The *Vm* system is characterized by three singular points (two stable and one a saddle point) whereas the full HH system has only a single stable singular point.

It is the saddle point which makes the two-variable approximation convenient for the calculation of threshold fluctuations. A saddle-point singular point always gives rise to a threshold separatrix dividing the phase plane into two distinct families of trajectories. As seen in Fig. 2, in the absence of a persistent stimulus, phase trajec-

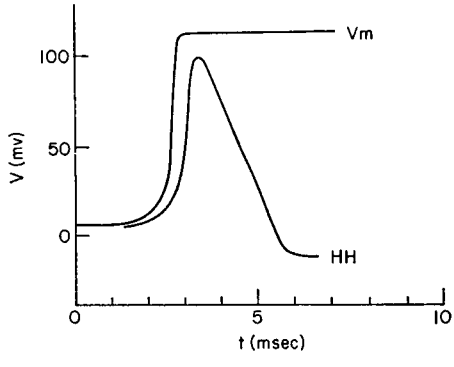

FIGURE 1 *c* Comparison of *Vm* and HH action potentials.

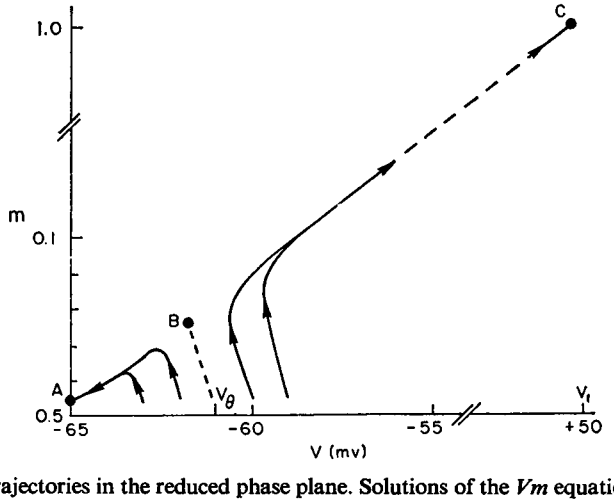

FIGURE 2 Trajectories in the reduced phase plane. Solutions of the *Vm* equations for $I = 0$ are replotted in the *Vm* plane. The points *A*, *B*, and *C* are the singular points. The point *A* corresponds to the normal resting state, and *C* to the "plateau" action potential. The point *B* is the threshold singular point and the dashed line is the threshold separatrix.

tories originating from the left of the separatrix return to the resting singular point A, whereas trajectories starting from the right terminate at the excited singular point C. Since the events represented by the trajectories of the Vm system fall into two distinct classes of outcomes, the system lends itself easily to probabilistic calculations.

Our discussion of threshold can be simplified by changing the usual notation. Referring to the equivalent circuit of Fig. 3, we can define the fundamental rate constants of the two-variable system as:

$$\gamma_0 = C^{-1}(g_K n_\infty^4(V_r) + g_L), \tag{4a}$$

$$\gamma_1 = C^{-1} g_{Na} h_\infty(V_r), \tag{4b}$$

$$\lambda(V) = 1/\tau_m(V), \tag{4c}$$

where V_r is the resting potential.

We define the effective emf's of the system as:

$$V_0 = (g_K n_\infty^4(V_r)V_K + g_L V_L)/(g_K n_\infty^4(V_r) + g_L), \tag{5a}$$

$$V_1 = V_{Na}, \tag{5b}$$

and the external driving forces as:

$$J = C^{-1}I. \tag{5c}$$

Further we wish to introduce a dimensionless conductance variable σ as:

$$\sigma \approx m^3 \text{ (HH), or}$$

$$\sigma \approx m^2 \text{ (FH).} \tag{6a}$$

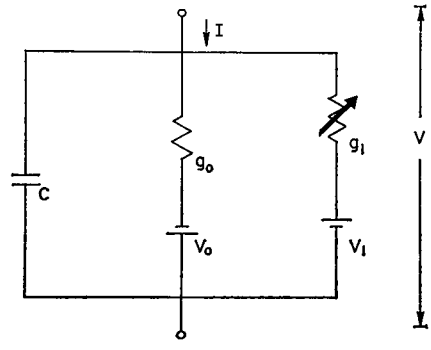

FIGURE 3 Approximate equivalent circuit for the $V\sigma$ system. All of the slowly varying and constant conductances are represented by g_0. The Na path is represented by g_1. The function σ represents Na activation as explained in the text. The parameters of the figure are defined in terms of the usual axon parameters in equations 4, 5, and 6.

The steady-state value of σ is given by the function

$$\sigma_\infty(V) = [m_\infty(V)]^3_{HH} \text{ or } [m_\infty(V)]^3_{FH} . \qquad (6b)$$

That $\sigma_\infty(V)$ is a natural variable for the excitable system can be seen in Fig. 4. Here we have plotted $\sigma_\infty(V)$ obtained from data on the squid, frog, and toad. The $m_\infty(V)$ functions found in the literature (Hodgkin and Huxley, 1952; Frankenhaeuser and Huxley, 1964; Dodge, 1963) have been fit empirically by different functional forms for these different preparations; however, we see from Fig. 4 that $\sigma_\infty(V)$ fits all the preparations with the same function. Thus, the conductance variable is more likely to be a universal quantity than is $m_\infty(V)$, and the use of conductance as a state variable avoids the unlikely suggestion that different preparations obey fundamentally different kinetics.

In terms of the new notation, equations 1–3 take the following simplified form:

$$\frac{dV}{dt} = J - \gamma_0(V - V_0) - \gamma_1\sigma(V - V_1) , \qquad (7)$$

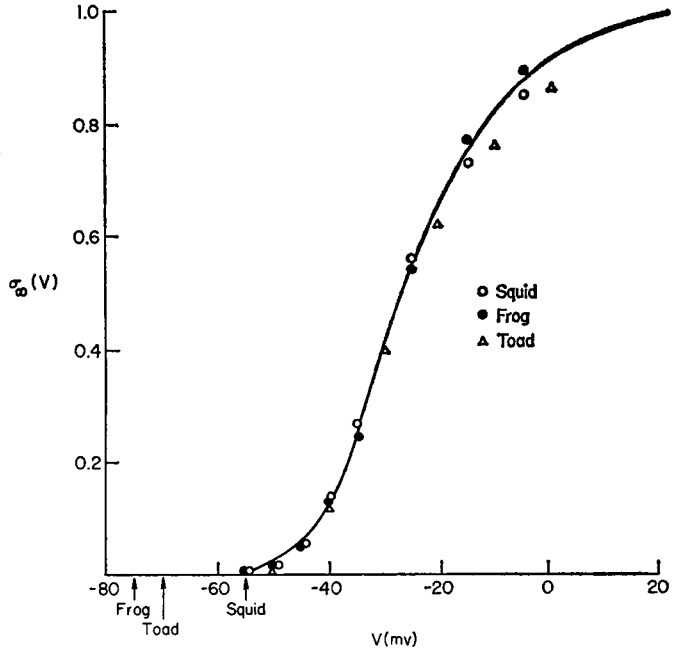

FIGURE 4 Normalized voltage-dependent conductance. The conductance function $\sigma_\infty(V)$ represents the Na activation of an axon in the absence of inactivation. Experimental data for different axon preparations have been plotted on an absolute voltage scale (rather than relative to the resting potential). Experimental data: ○, squid giant axon (Hodgkin and Huxley, 1952); △, toad node of Ranvier (Frankenhaeuser and Huxley, 1954); ●, frog node of Ranvier (Dodge, 1963).

and

$$\frac{d\sigma}{dt} = \phi(V, \sigma). \tag{8}$$

Here ϕ is a function whose properties are chosen to duplicate the kinetics of the Na conductance. For computational purposes, we shall take equation 8 to be a transcription of the *Vm* equations, with

$$\phi(V, \sigma) = 3\lambda(V)\sigma^{2/3}[\sigma_\infty(V)^{1/3} - \sigma^{1/3}]. \tag{9}$$

Much of the noise treatment, however, can be carried out without reference to the explicit form of $\phi(V, \sigma)$. In treating the problem of conductance fluctuations in the following paper, we will use a particular stochastic model for the voltage-dependent conductance.[1] Thus, rather than restrict ourselves to the form of equation 9, we will let the supposed physics of the Na conductance model determine the form of $\phi(V, \sigma)$. Table I gives the numerical values of the parameters of equations 7 and 8 for three axons which have been extensively studied experimentally by the voltage clamp technique.

III. $V\sigma$ EQUATIONS WITH NOISE SOURCES

When noise is present V and σ become fluctuating quantities. The deterministic phase trajectories must be replaced by a time-varying probability distribution for the position of the system in the $V\sigma$ plane. The motion of a phase point in the presence of noise can be considered as a random walk carrying the phase point back and forth across the threshold separatrix.

If we assume that the stimulus is of very short duration, then the immediate effect of the stimulus is to move the phase point parallel to the V-axis into the region of the separatrix. After the stimulus is shut off, the phase point drifts along the separatrix up to the region of the saddle point (see Fig. 2). Near the saddle point, the phase trajectories are repelled, causing the phase point to accelerate away from the saddle-point region towards one of the stable singular points. This acceleration dominates over the random forces and the system has only a vanishingly small probability of returning to the separatrix region. Thus, for the $V\sigma$ equations, the probability that the nerve has fired is equal to the probability that, after a long time, the phase point is found on the suprathreshold side of the se paratrix.

We represent the effects of noise by equivalent random forces for the sources of

[1] A particularly simple example of an alternative form for $\phi(V, \sigma)$ is

$$\phi(V, \sigma) = A\sigma - B\sigma^2 = 3\lambda(V)\sigma[1 - \sigma/\sigma_\infty(V)].$$

With this form, equation 8 becomes a modification of the "logistic" equation (Davis, 1960), which yields time-delay kinetics without having to raise the fundamental variable to a higher power.

TABLE I

PARAMETERS USED IN COMPUTATIONS

Parameter	Squid (HH)	Toad node (FH)	Frog node (Hille)
γ_0, 10^3 sec^{-1}	0.56	15.2	2.5
γ_1, 10^3 sec^{-1}	59.6	144.4	48.5
γ_0/γ_1	0.0094	0.105	0.052
V_0, mv	−65	−70	−75
V_1, mv	50	53	48
λ, 10^3 sec^{-1}	4.0	16.3	10.0
Temperature, °C	6.3	23	22

voltage or conductance fluctuations. Such random forces are generally called Langevin forces (Lax, 1966; Chandrasekhar, 1943). In the presence of the fluctuating forces, the $V\sigma$ equations become

$$\frac{dV}{dt} = J - \gamma_0(V - V_0) - \gamma_1\sigma(V - V_1) + F_V(\langle\sigma\rangle, t) , \tag{10}$$

$$\frac{d\sigma}{dt} = \phi(V, \sigma) + F_\sigma(\langle V\rangle, t) . \tag{11}$$

Here F_V and F_σ, the Langevin forces, are random time functions but may also depend upon the mean value of voltage $\langle V(t)\rangle$ or conductance $\langle\sigma(t)\rangle$. This dependence can be thought of as a way of taking the nonlinearity of the system into account. Thus, for example, if the term F_V represented thermal voltage noise, its magnitude would depend upon the membrane conductance via the fluctuation-dissipation theorem (Callen and Welton, 1951).

Let us next expand equations 10 and 11 in the neighborhood of the threshold singular point B. It is convenient to express the equations in terms of dimensionless variables. Letting

$$\epsilon = (V - V_B)/V_1, \tag{12a}$$

and

$$\mu = \sigma - \sigma_B, \tag{12b}$$

we obtain the equations:

$$\frac{d\epsilon}{dt} = A_{11}\epsilon + A_{12}\mu + \cdots + V_1^{-1}F_V(\sigma_B, t) + \cdots \tag{13a}$$

$$\frac{d\mu}{dt} = A_{21}\epsilon + A_{22}\mu + \cdots + F_\sigma(V_B, t) + \cdots . \tag{13b}$$

Using equation 9, the coefficients A_{ij} are given explicitly as

$$A_{11} = -(\gamma_1\sigma_B + \gamma_0),$$
$$A_{12} = \gamma_1 V_1^{-1}(V_1 - V_B),$$
$$A_{21} = \lambda(V_B)V_1\left[\frac{\partial\sigma_\infty(V)}{\partial V}\right]_{V=V_B},$$
$$A_{22} = -\lambda(V_B). \tag{14}$$

In the linearized equations (equations 13), the coupling terms A_{12} and A_{21} preserve the character of the nonlinear circuit. Indeed, if this pair of first-order equations were rewritten as a single second-order differential equation, the circuit so represented would be seen to have a negative dynamic resistance in the saddle-point region.

Equations 13 are most easily solved by a transformation of variables which diagonalizes the matrix of the coefficients A_{ij}. Thus we can find a matrix Z_{ij} such that the variables y_i, defined as

$$y_i = Z_{i1}\epsilon + Z_{i2}\mu, \qquad i = 1, 2, \tag{15}$$

are solutions of equations 13 having the form

$$y_1(t) = y_1(0)e^{p_i t} + \int_0^t e^{p_i(t-s)}[Z_{i1}F_\epsilon(s) + Z_{i2}F_\mu(s)]\,ds. \tag{16}$$

Here, the rate constants p_i are the eigenvalues of A_{ij} and are given by:

$$p_1, p_2 = \tfrac{1}{2}(A_{11} + A_{22}) \pm \tfrac{1}{2}[(A_{11} - A_{22})^2 + 4A_{12}A_2]^{1/2}. \tag{17}$$

The matrix Z_{ij} needed to effect the transformation is given by:

$$Z_{11} = \frac{A_{11} - p_2}{p_1 - p_2}\left[1 + \left(\frac{A_{11} - p_1}{A_{12}}\right)^2\right]^{1/2}, Z_{12} = \frac{A_{12}}{p_1 - p_2}\left[1 + \left(\frac{A_{11} - p_1}{A_{12}}\right)^2\right]^{1/2},$$
$$Z_{21} = \frac{A_{11} - p_1}{p_1 - p_2}\left[1 + \left(\frac{A_{11} - p_2}{A_{12}}\right)^2\right]^{1/2}, Z_{22} = A_{12}\left[1 + \left(\frac{A_{11} - p_2}{A_{12}}\right)^2\right]^{1/2}. \tag{18}$$

The principal axes for the $V\sigma$ equations (for the case of the node of Ranvier) are shown in Fig. 5. As is seen in the figure, the principal axes coincide with the separatrices in the neighborhood of point B. Since the threshold separatrix coin cides with the y_2-axis, the projection of the motion of the phase point along the y_1-direction is a measure of the departure from the separatrix. Note, however, that the projections described by Z_{ij} are not necessarily orthogonal.

The principal-axis transformation has reduced our problem to a one-dimensional

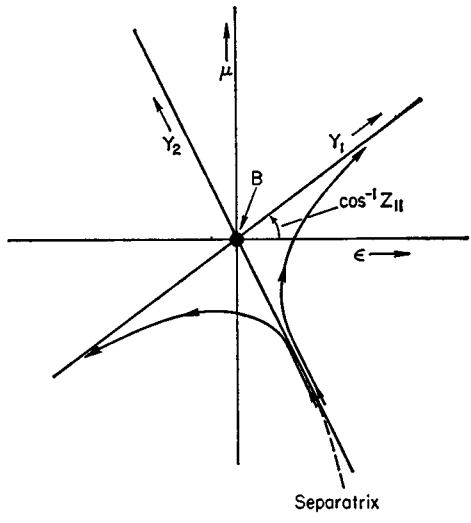

FIGURE 5 Principal axes of the FH equations in the neighborhood of the threshold singular point B. The y_2-axis coincides with the threshold separatrix in this region. The y_1-axis is the asymptote which all the phase trajectories approach upon leaving the threshold region.

random walk in the y_1-direction. Letting

$$X(t) = Z_{11}F_\epsilon(t) + Z_{12}F_\mu(t), \tag{19}$$

the integral of equation 16 can be rewritten as:

$$Y(t) = y_1(t) - y_1(0)e^{p_1 t} = \int_0^t e^{p_1(t-s)}X(s)\,ds. \tag{16'}$$

Generally, the function $X(t)$ represents the result of many small independent random events. For such a case, $X(t)$ is a gaussian random variable. It follows (Chandrasekhar, 1943) that the time integral $Y(t)$ also obeys a gaussian distribution. Thus, the probability that $y_1(t)$ departs from its mean by an amount Y at time t is given by

$$P(Y, t) = (2\pi\langle Y^2\rangle)^{-1/2} \exp\ (-Y^2/2\langle Y^2\rangle), \tag{20}$$

where the angular brackets denote an expectation value. The expectation value of Y^2 can be expressed in terms of the joint expectation of the variable X taken with itself at a different time. From equation 20 one finds

$$\langle Y^2\rangle = e^{2p_1 t}\int_0^t\int_0^t e^{-p_1(\xi+\eta)}\,\langle X(\xi)X(\eta)\rangle\,d\xi\,d\eta. \tag{21}$$

From equation 20 and 21, we can calculate the probability of firing when given an initial displacement $y_1(0)$. The probability of firing is equal to the probability

that $y_1(t) > 0$ when $t \to \infty$. Hence,

$$P[\text{fire} \mid y_1(0)] = \lim_{t \to \infty} \int_{-y_1(0) \exp(p_1 t)}^{\infty} P(Y, t)\, dY, \tag{22}$$

or

$$P[\text{fire} \mid y_1(0)] = \tfrac{1}{2}[1 + \text{erf}\ (y_1(0)/\sqrt{2}\, D^{1/2})]. \tag{23}$$

Here erf (x) is defined as

$$\text{erf}\ (x) = (2/\sqrt{\pi}) \int_0^x e^{-\eta^2}\, d\eta,$$

and D is defined as

$$D = \int_0^{\infty} \int_0^{\infty} e^{-p_1(\xi+\eta)} \langle X(\xi) X(\eta) \rangle\, d\xi\, d\eta. \tag{24}$$

Equation 23 is the desired relation between the probability of firing and the initial state of the system; however, we wish to rewrite the equation in terms of an observable parameter instead of $y_1(0)$. For the case of a short-duration stimulus, $y_1(0)$ can be simply related to the initial voltage displacement from threshold; from equation 15, we see that $y_1(0) = Z_{11}\epsilon(0)$. Thus, if we define the initial voltage displacement from threshold as

$$\Delta V = V - V_\theta,$$

and substitute from equation 12 a for $\epsilon(0)$, equation 23 becomes

$$P(\text{fire} \mid \Delta V) = \tfrac{1}{2}[1 + \text{erf}\ (\Delta V Z_{11}/V_1 \sqrt{2}\, D^{1/2})]. \tag{25}$$

Equation 25 expresses the probability of firing as an integrated gaussian distribution function of the stimulus strength. This is in agreement with the experimental curve (Pecher, 1939; Ten Hoopen and Verveen, 1963). In the experimental papers, a normalized parameter defined as the width of the distribution divided by the threshold value of stimulus was used for comparing results. This parameter is called the relative spread (Ten Hoopen and Verveen, 1963). Setting the argument of erf $(-)$ equal to unity in equation 25, we can readily obtain an explicit expression for the relative spread as

$$R = \sqrt{2}\, D^{1/2} V_1 / Z_{11}(V_\theta - V_0) = \frac{\sqrt{2}\, D^{1/2}}{Z_{11}} \frac{V_1}{V_\theta^*}, \tag{26}$$

where V_θ^* is the threshold depolarization measured from rest (for a short-duration stimulus). One characteristic which has been noted from threshold fluctuation ex-

periments is that R is approximately constant when the stimulus duration is varied. This property will be discussed further in the next section.

IV. OTHER CHARACTERISTICS OF THE FLUCTUATIONS

In the previous section we derived the formula for the probability of firing in response to a short-duration stimulus. Implicit in the derivation is the assumption that within a certain crucial region of phase space, where sub- and suprathreshold trajectories begin to diverge from each other, the full set of HH equations can be approximated by the $V\sigma$ equations. In this way the topological features of the $V\sigma$ phase plane, i.e., threshold singular point and separatrix, are employed as the basis of the calculation. For stimuli other than short shocks to the threshold separatrix, we must also consider the effects of noise operating on the system during motion of the phase point towards the threshold separatrix. Considerable time may be spent in reaching the separatrix and equation 25 must be modified to take such past history into account. Although a precise description of the motion of the phase point during stimulation would require the full set of HH equations, we here describe several aspects of excitability fluctuations which can be treated by the approximate model introduced in the previous sections. We focus upon three characteristics which have been studied experimentally on nerve fibers (Ten Hoopen and Verveen, 1963):

(a) the dependence of the relative spread upon stimulus current,

(b) the probability of firing as a function of stimulus duration for a fixed current, and

(c) the distribution of latency times for various stimuli.

Any method of generalizing equation 25 to take account of the past history of motion in the phase plane is equivalent to a convolution of the distribution of equation 25 with another distribution representing the spread of phase positions accumulated before the phase point entered the singular-point region. For example, let us assume that the effect of noise during the subthreshold motion can be summarized by replacing the initial position $y_1(0)$ by a gaussian distribution of initial values,

$$P[y_1(0) = \xi] = (2\pi A^2)^{-1/2} \exp\left\{-\frac{[\xi - y_1(0)]^2}{2A^2}\right\}. \tag{27}$$

The parameter A represents the width resulting from past history.

The distribution of equation 23 must be convoluted with that of equation 27. Since the convolution of two gaussians is a gaussian, we immediately obtain a result similar to equation 25 but depending on past motion of the system,

$$P(\text{fire} \mid y_1(0), A) = \tfrac{1}{2}\{1 + \text{erf}\,[y_1(0)/2(A^2 + D)^{1/2}]\}. \tag{28}$$

Thus the problem of generalizing equation 25 has been reduced to that of calculating A in some reasonable manner.

Invariance of the Relative Spread

One method of studying the past history of motion in the phase plane is to use the linearized $V\sigma$ equations themselves as a rough approximation to the dynamics of the system during the approach to the separatrix. Employing this approximation, we can demonstrate the constancy of the relative spread.

In the presence of a stimulus $J(t)$, equation 16 becomes

$$y_1(t) = y_1(0)e^{p_1 t} + (Z_{11}/V_1)\int_0^t e^{p_1(t-s)}J(s)\,ds + \int_0^t e^{p_1(t-s)}X(s)\,ds. \quad (29)$$

Here $t = 0$ denotes the time when the signal is just turned on, and $y_1(0)$ is some position on the negative side of the separatrix ($y_1 = 0$ line). For a constant value of J, and in the absence of noise, we have

$$\langle y_1(t)\rangle = y_1(0)e^{p_1 t} + (Z_{11}/p_1V_1)J(e^{p_1 t} - 1). \quad (30)$$

By setting $\langle y_1(t)\rangle = 0$ we can solve for the time T needed to reach the separatrix as a function of J. This leads to an expression relating the threshold value of J to a given pulse duration T,

$$J_\theta = \frac{-p_1 y_1(0)V_1 Z_{11}^{-1}}{1 - e^{-p_1 T}}. \quad (31)$$

The quantity in the numerator of equation 31 can be redefined to be the minimum (rheobase) stimulating current J_{Rh}. Consequently, equation 31 is the strength-duration relation for the linearized $V\sigma$ model, and is seen to have the form of the classical Lapicque's law (Cole, 1968).

Let us consider a value of J differing from J_θ, which we choose to write as

$$J = J_\theta(1 + \Delta). \quad (32)$$

From equation 29 we write the position of the phase point at a time $t \geq T$ as

$$y_1(t) = y_1(0)e^{p_1 t} + \frac{Z_{11}J}{V_1 p_1}(1 - e^{-p_1 T})e^{p_1 t} + \int_0^t e^{p_1(t-s)}X(s)\,ds. \quad (33)$$

Substitution from equations 31 and 32 gives

$$y_1(t) = \left[\frac{Z_{11}J_{Rh}\Delta}{V_1 p_1} + \int_0^t e^{-p_1 s}X(s)\,ds\right]e^{p_1 t}. \quad (34)$$

We have now arrived at an expression having the same form as equation 16. Therefore, we can follow the steps which led to equation 23 and reach a general expression

for the probability of firing in response to a pulse of arbitrary duration,

$$P(\text{fire} \mid \Delta) = \tfrac{1}{2}\left\{1 + \text{erf}\left[\frac{Z_{11}J_{Rh}\Delta}{V_1 p_1 (2D)^{1/2}}\right]\right\}. \qquad (35)$$

Equation 35 leads to an explicit expression for the relative spread. Setting the argument of the error function equal to unity and solving the resulting equation for Δ, we obtain

$$R = p_1 V_1 (2D)^{1/2} / J_{Rh} Z_{11}. \qquad (36)$$

Here, R is seen to be independent of stimulus duration (Fig. 6).

Such invariance of the relative spread has been noted experimentally both for nerves and electronic models (Ten Hoopen and Verveen, 1963). We conclude from our ability to derive this result by such a crude approximation that the distortion of phase trajectories by linearization does not change their relative topological character. In particular, the relative separation of the points where trajectories cross the separatrix is preserved. Thus, we suspect that the invariance of the relative spread is a rather nonspecific property of certain broad classes of triggerable systems. It does not depend either on the details of the dynamics or on the nature of the noise source, provided only that the noise intensity is relatively small and that a strength-duration relation of the form of equation 31 is obeyed.

Duration-Probability Relation

By a slight modification of the foregoing argument, we can derive the relation for the probability of firing at a given stimulus strength as a function of stimulus duration.

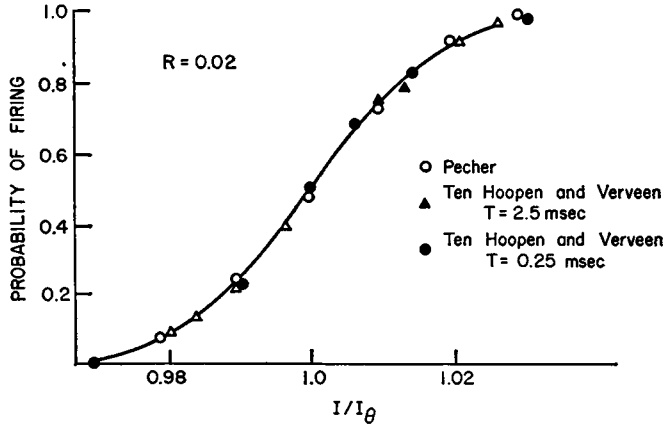

FIGURE 6 Probability of firing as a function of stimulus strength. The solid curve is plotted from equation 35, with the relative spread taken to be 0.02. The data of Ten Hoopen and Verveen, pertaining to the same nerve, illustrate the invariance of the relative spread for varying pulse durations.

For a given value of J, let T be the duration of the stimulating pulse and T_θ be the time to reach the separatrix. From equations 31 and 33, we obtain

$$y_1(t) = \left[\frac{Z_{11}J}{V_1 p_1}\left(e^{-p_1 T_\theta} - e^{-p_1 T}\right) + \int_0^t e^{p_1(t-s)}X(s)\,ds\right]e^{p_1 t}. \qquad (37)$$

Again following the argument which led to equation 23, the probability of firing is given as

$$P(\text{fire}\,|\,T, J) = \tfrac{1}{2}\left\{1 + \text{erf}\left[\left(\frac{Z_{11}J}{p_1 V_1 (2D)^{1/2}}\right)\left(e^{-p_1 T_\theta} - e^{-p_1 T}\right)\right]\right\}. \qquad (38)$$

Using equations 31 and 36, this expression can be rewritten as

$$P(\text{fire}\,|\,T, J) = \tfrac{1}{2}\left\{1 + \text{erf}\left[\frac{1}{R}\left(\frac{J}{J_{\text{Rh}}} - 1\right)\left(1 - e^{-p_1(T-T_\theta)}\right)\right]\right\}. \qquad (39)$$

A family of these duration-probability curves is shown in Fig. 7. The most striking aspect of these theoretical curves is the extreme sensitivity of the shape of the individual curves to small changes in J, a feature which can be seen also in the experimental curves of Ten Hoopen and Verveen (1963; Fig. 3).

Latency Distribution

A similar derivation, based on subthreshold motion in the phase plane, can be given for the latency distribution; however, the latency distribution can be derived more easily by using the $V\sigma$ equations to obtain an expression relating latency to stimulus strength and then convoluting with a hypothetical distribution of stimuli whose width is of the same order of magnitude as the relative spread.

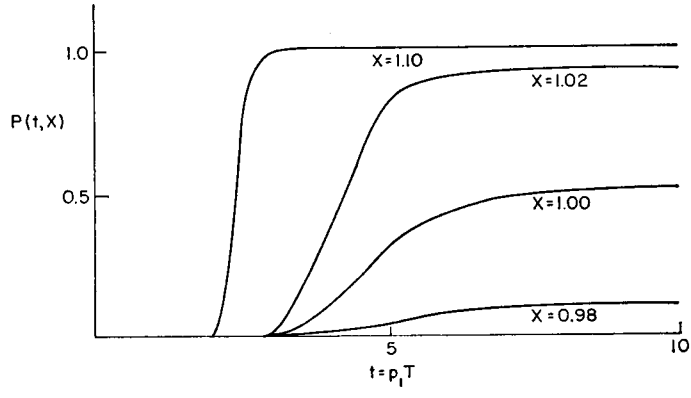

FIGURE 7 Firing probability vs. pulse duration, $P(\text{fire}\,|\,T, J)$, plotted from equation 39 with R taken to be 0.02. The dimensionless variables X and t are defined as $X = J/J_{\text{Rh}}$ and $t = p_1 T$. These curves show the same sensitivity to stimulating current as do the experimental data of Ten Hoopen and Verveen (1963, Fig. 3).

The latency time is usually defined as the time to reach the peak of the action potential; however, since the $V\sigma$ system displays plateau action potentials, we here define the latency as the time needed to reach some fixed distance from the excited singular point. Designating this criterion by an arbitrary barrier at $y_1 = y^*$, we can solve equation 34 for the time t^* needed to reach y^* in the absence of noise. We find

$$t^*(\Delta) = p_1^{-1} \log_e (b/\Delta), \tag{40}$$

where

$$b = y^* V_1 p_1 / Z_{11} J_{Rh}. \tag{41}$$

Let us now assume that a nominal stimulus Δ must be replaced by a small spread of stimuli, described by

$$W(X) = \alpha \pi^{-1/2} \exp - [\alpha (X - \Delta)]^2. \tag{42}$$

Defining $\eta = t^*(X)$ as the random variable for the latency, we use the transformation (Stratonovich, 1963)

$$W(\eta) = W[X(\eta)] \left| \frac{dX}{d\eta} \right|_{x=x(\eta)} \tag{43}$$

to obtain the distribution of latencies,

$$W(\eta) = \alpha b p_1 \pi^{-1/2} e^{-p_1 \eta} e^{-(\alpha b)^2 (e^{-p_1 \eta} - \Delta/b)^2}. \tag{44}$$

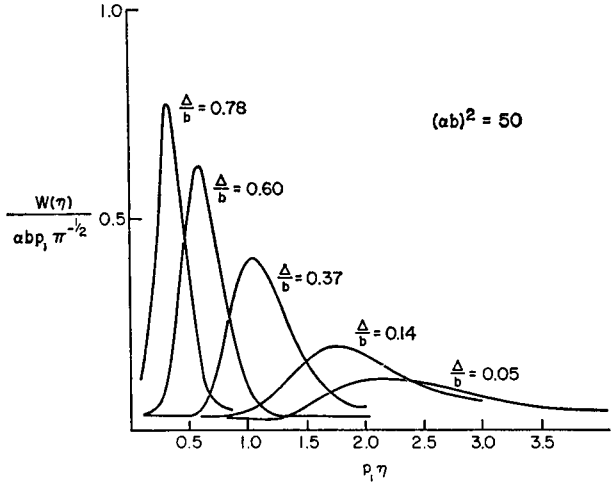

FIGURE 8 Distribution of latency times as a function of normalized stimulus intensity Δ. The scale of latency times has also been normalized by multiplying by the rate constant p_1. This family of curves was obtained from equation 44, using the value $(\alpha b)^{-2} = 0.02$. An experimental family of latency histograms is given by Ten Hoopen and Verveen (1963, Fig. 4).

This latency distribution is plotted in Fig. 8, where we see the characteristic skewness and varying width of the histograms. These properties are immediate consequences of the steep falloff of the latency function $t^*(\Delta)$ with increasing stimulus strength (see equation 40).

V. REMARKS

More general insight into the conditions under which the $V\sigma$ approximation is a good quantitative description of threshold can be obtained by considering the effects of leakage current. Note from Table I that the parameter γ_0, representing the leakage conductance, varies greatly from one preparation to another. The rate constant γ_0 is associated with the discharge of the membrane capacitance via the time-independent leakage conductance. All of the other conductance parameters are autonomous functions of voltage, and their changes lag behind initial changes in voltage. Thus, it is leakage which sets the time scale for the threshold phenomenon.

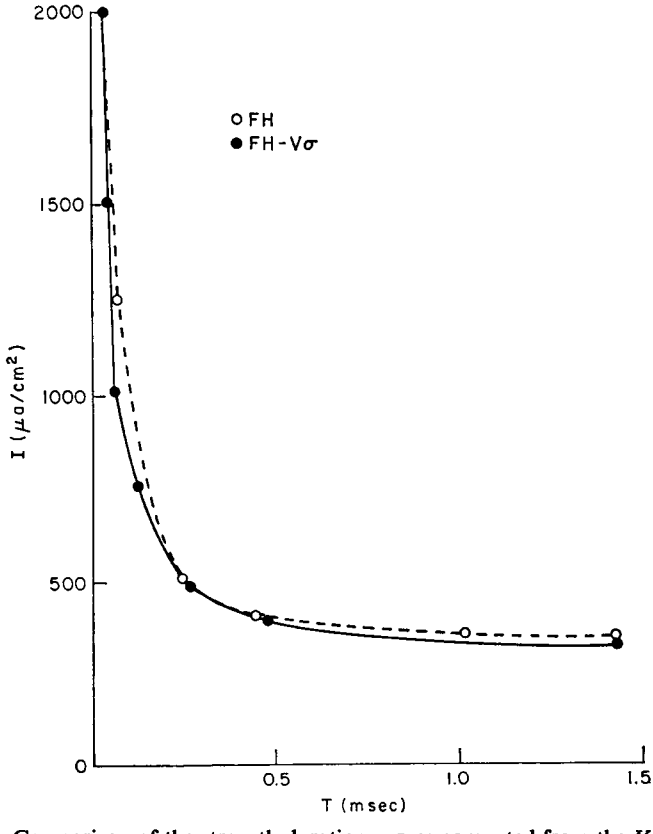

FIGURE 9 *a* Comparison of the strength-duration curves computed from the $V\sigma$ equations with those resulting from exact FH equations for the node of Ranvier, *Xenopus laevis*. Solutions of exact FH equations are from Frankenhaeuser (1965).

When leakage is high (as in the case of node), motion along the separatrix at the termination of the stimulus is rapid, and the threshold condition is determined by the competition of capacitative discharge and sodium-current buildup. On the other hand, when leakage is low (as in the case of the squid giant axon) the $V\sigma$ phase trajectories remain in the separatrix region for a time long enough for the recovery variables to come into play, and the two-variable system does not adequately approximate the threshold properties.

To illustrate the importance of the relative magnitude of the leakage, we have calculated the strength-duration curves in the absence of noise for the $V\sigma$ modifications of both the HH (low leakage) and FH (high leakage) equations. These curves are shown, together with the curves calculated from the full HH and FH equations, in Figs. 9 *a* and 9 *b*. Comparing the curves, we see that neglect of the recovery variables introduces a large error only when leakage is low. Threshold fluctuation experiments have been performed mainly on noded nerves, because the node of Ranvier is an isolated area of excitable membrane small enough to exhibit measurable fluctuations.

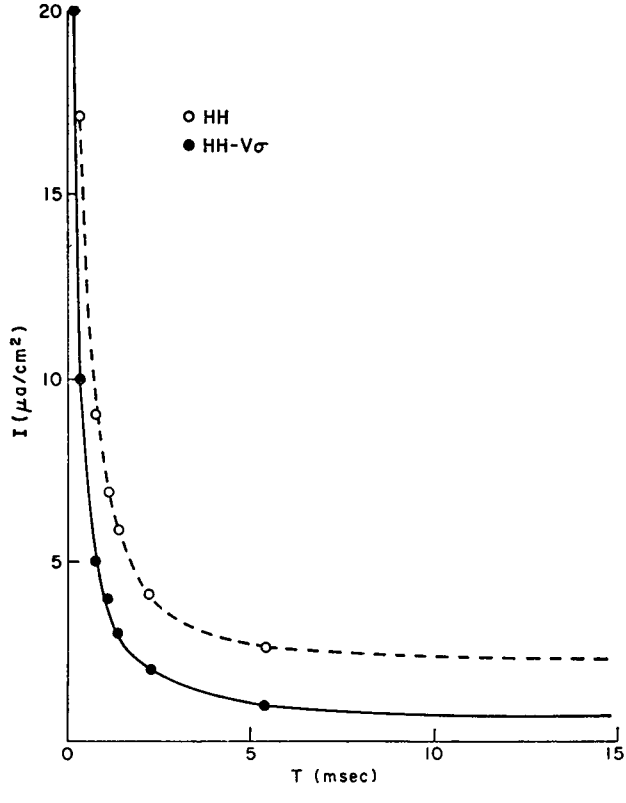

FIGURE 9 *b* Comparison of the strength-duration curves computed from the $V\sigma$ equations with those resulting from exact HH equations for squid giant axon. Numbers for the exact HH solutions have been taken from Noble and Stein (1966); see also Cole (1968).

Nodes are high-leakage preparations, for which we expect the $V\sigma$ approximation to be quantitatively applicable.

It might be surprising that the two-variable description of threshold fluctuations works as well as it does, in view of the topological dissimilarities between the reduced system and the full HH system. One important difference between the $V\sigma$ and HH equations, which arises from the omission of the recovery variables, is that the latency values possible for $V\sigma$ solutions are unbounded, in contrast to the upper bound of about 6 msec predicted from the HH equations. It might be supposed that such spurious long-latency trajectories would greatly affect the probability distributions; however, by calculating the diffusion time for a phase point to leave the separatrix region when noise is present, one can show that the long-latency trajectories are really very sparsely populated. For example, using the experimental value of 3% threshold fluctuations as a guide to estimating the strength of the noise source, we have calculated that the time for phase points starting at the separatrix to diffuse out of the near-separatrix region of long latencies is less than 0.1 msec.

Also, intermediate voltage responses of the HH system are excluded in the $V\sigma$ approximation. Graded responses have recently been demonstrated both experimentally and theoretically for the squid giant axon at high temperatures (Cole et al., 1970). Such responses need not be considered here, however, because, under usual experimental conditions, the range of stimulus intensity for which the graded responses may be observed is far more narrow than the spread of initial conditions caused by thermal noise (FitzHugh, 1955; Cole, 1968).

Received for publication 16 April 1971.

REFERENCES

BLAIR, E. A., and J. ERLANGER. 1932. *Proc. Soc. Exp. Biol. Med.* **29**:926.

CALLEN, H. B., and T. A. WELTON. 1951. *Phys. Rev.* **83**:34.

CHANDRASEKHAR, S. 1943. *Rev. Mod. Phys.* **15**:1.

COLE, K. S. 1968. Membranes, Ions, and Impulses. University of California Press, Berkeley, Calif.

COLE, K. S., R. GUTTMAN, and F. BEZANILLA. 1970. *Proc. Nat. Acad. Sci. U.S.A.* **65**:884.

DAVIS, H. T. 1960. Introduction to Nonlinear Differential and Integral Equations. United States Atomic Energy Commission, United States Government Printing Office, Washington, D. C.

DODGE, F. 1963. A study of ionic permeability changes underlying excitation in myelinated nerve fibers of the frog. Ph.D. Thesis. The Rockefeller University, New York.

FITZHUGH, R. 1955. *Bull. Math. Biophys.* **17**:257.

FITZHUGH, R. 1961. *Biophys. J.* **1**:445.

FITZHUGH, R. 1969. Biological Engineering. H. P. Schwan, editor. McGraw-Hill Book Company, New York. 1.

FRANKENHAEUSER, B. 1965. *J. Physiol. (London).* **180**:780.

FRANKENHAEUSER, B., and A. F. HUXLEY. 1964. *J. Physiol. (London).* **171**:302.

GASTWIRTH, J. L. 1967. A Renewal Theoretic Approach to a First Passage Time Problem Occurring in a Neuron Firing Model. Technical Report No. 77. Department of Statistics, The Johns Hopkins University, Baltimore.

GOLDMAN, D. E. 1943. *J. Gen. Physiol.* **27**:37.

HODGKIN, A. L., and A. F. HUXLEY. 1952. *J. Physiol. (London).* **117**:500.

LANDAHL, H. D. 1941. *Bull. Math. Biophys.* **3**:141.

LAX, M. 1966. *Rev. Mod. Phys.* **38**:541.
MONNIER, A. M., and H. H. JASPER. 1932. *C. R. Soc. Biol.* **110**:547.
NOBLE, D., and R. B. STEIN. 1966. *J. Physiol. (London).* **187**:129.
PECHER, C. 1939. *Arch. Int. Physiol.* **49**:129.
POUSSART, D. 1969. *Proc. Nat. Acad. Sci. U.S.A.* **64**:95.
STEIN, R. B. 1967. *Biophys. J.* **7**:37.
STRATONOVICH, R. L. 1963. Topics in the Theory of Random Noise. Gordon & Breach, Science Publishers, Inc., New York.
TEN HOOPEN, M., and A. A. VERVEEN. 1963. Proceedings of International Conference on Cybernetics in Medicine. N. Wiener and J. P. Schadé, editors. Elsevier Publishing Co., Amsterdam.
VERVEEN, A. A., and H. E. DERKSEN. 1968. *Proc. I.E.E.E. (Inst. Elec. Electron. Eng.).* **56**:906.